

The Left-Right asymmetry of top quarks in associated top–charged Higgs bosons at the LHC as a probe of the $\tan\beta$ parameter

J. Baglio¹, M. Beccaria², A. Djouadi^{1,3}, G. Macorini^{2,4},
E. Mirabella⁵, N. Orlando²,
F.M. Renard³, C. Verzegnassi⁴,

¹ Laboratoire de Physique Théorique, Université Paris XI et CNRS, Orsay, France.

² Dipartimento di Fisica, Università del Salento and INFN, Sezione di Lecce, Italy.

³ Theory Unit, CERN, 1211 Genève 23, Switzerland.

⁴ Niels Bohr International Academy and Discovery Center, Blegdamsvej 17 DK-2100 Copenhagen, Denmark

⁵ Institut de Physique Théorique, CEA–Saclay, F–91191 Gif sur Yvette, France.

⁶ Laboratoire Univers et Particules, U. Montpellier II, France.

⁷ Dipartimento di Fisica Teorica, Università di Trieste and INFN Sezione di Trieste, Italy.

Abstract

Many extensions of the Standard Model involve two Higgs doublet fields to break the electroweak symmetry, leading to the existence of three neutral and two charged Higgs particles. In particular, this is the case of the Minimal Supersymmetric extension of the Standard Model, the MSSM. A very important parameter is $\tan\beta$ defined as the ratio of the vacuum expectation value of the two Higgs doublets. In this paper we focus on the left-right asymmetry in the production of polarised top quarks in association with charged Higgs bosons at the LHC. This quantity allows for a theoretically clean determination of $\tan\beta$. In the MSSM, the asymmetry remains sensitive to the strong and electroweak radiative corrections and, thus, to the superparticle spectrum. Some possible implications of these results are discussed.

1. Introduction

A widely studied extensions of the Standard Model (SM) are the two-Higgs doublet model (2HDM) in which two SU(2) doublets of complex scalar fields are introduced to break the electroweak symmetry [1]. In particular the Higgs sector of the Minimal Supersymmetric extension of the Standard Model (MSSM) [2] is a type II 2HDM. These models lead to the existence of five scalar particles, two CP-even bosons (h, H) a CP-odd one (A) and two charged particles (H^\pm). The Higgs sector of a 2HDM model is described by six parameters. They can be chosen to be the four masses of the Higgs particles, the mixing angle α in the CP-even Higgs sector and the ratio $\tan\beta$ of the vacuum expectation values of the two Higgs doublets. In the MSSM these parameters are no longer independent. The two parameters describing the Higgs sector of the MSSM may be taken to be the charged Higgs mass M_{H^\pm} and $\tan\beta$. The precise determination of these parameters is of great importance to identify the underlying model and to determine its basic features.

Once the Higgs bosons have been produced, their mass can be measured looking at the kinematical distributions of the decays products [3]. In the MSSM the parameter $\tan\beta$ can be determined looking at the total cross section of processes involving Higgs bosons. For instance in the MSSM the total cross sections $pp(\bar{p}) \rightarrow H, A$ are proportional to $\tan^2\beta$ [4]. A measurement of the relevant production cross sections at the LHC, allows for a determination of $\tan\beta$ [5] with an uncertainty of the order of 30%.

Another interesting process is the production of the charged Higgs boson in association with a top quark in bottom-gluon fusion at hadron colliders [6–10]

$$bg \rightarrow tH^-, \quad \bar{b}g \rightarrow \bar{t}H^+, \quad (1)$$

in which the bottom quark is directly taken from the proton in a five flavor scheme. The cross section of this process is proportional to the square of the Yukawa coupling $g_{H^\pm tb}$. In type II 2HDMs $g_{H^\pm tb}$ reads as follows [1],

$$g_{H^\pm tb} = \frac{g}{\sqrt{2}M_W} V_{tb} \{ H^+ \bar{t} [m_b \tan\beta P_R + m_t \cot\beta P_L] b + \text{h.c.} \}, \quad (2)$$

where $g = e/s_W$ is the SU(2) coupling and $P_{L/R} = (1 \mp \gamma_5)/2$ are the chiral projectors. The Cabbibo-Kobayashi-Maskawa matrix element V_{tb} can be set, to a good approximation, to unity [11]. At tree-level the total production cross sections of the processes in eq. (1) are equal and proportional to $(m_t^2 \cot^2\beta + m_b^2 \tan^2\beta)$. They are significant both in the $\tan\beta \leq 1$ and in the $\tan\beta \gg 1$ regions¹. In type I 2HDMs, all fermions couple to only one Higgs field. The $g_{H^\pm tb}$ coupling has to be modified performing the substitution $m_b \tan\beta \rightarrow m_b \cot\beta$ in eq. (2). The sum of the total cross section of the two processes in eq. (1) is proportional to $\cot^2\beta$ and is enhanced for small $\tan\beta$ values only².

Besides the experimental uncertainties, the cross section measurement is plagued with various theoretical uncertainties [12]. The most important uncertainties are related to the dependence of the observables on the renormalisation and factorisation scales, as well as the

¹The total cross section exhibits a minimum at $\tan\beta = \sqrt{m_t/m_b} \approx 7$.

²In the MSSM the lower bound of the mass of h requires that $\tan\beta \gtrsim 2-3$ [2, 11]. In a general 2HDM $\tan\beta$ is less constrained. The region $0.2 \lesssim \tan\beta \lesssim 50$ is not ruled out and preserves the perturbativity of the Higgs Yukawa coupling (2).

dependence on the choice of the parton distribution functions (PDFs), and the related errors on the strong coupling constant α_s . These theoretical uncertainties can be of the order of 20 – 30% [5] and are a major source of error in the determination of $\tan\beta$ directly from the Higgs production cross section.

In this letter, we propose an alternative way to measure the parameter $\tan\beta$ which is free of these theoretical uncertainties. The method uses the left–right asymmetry constructed from the longitudinal polarisation of the top quarks produced in association with the charged Higgs bosons, the latter decaying via the clean and detectable $H^\pm \rightarrow \tau^\pm\nu$ decay channel. The polarisation asymmetry A_{LR}^t is defined as the difference of cross sections for the production of left–handed and right–handed top quarks divided by their sum³

$$A_{LR}^t \equiv \frac{\sigma_L - \sigma_R}{\sigma_L + \sigma_R}, \quad (3)$$

where $\sigma_{L/R}$ is the total hadronic cross section of the process of $t_{L/R}H^-$ associated production. The asymmetry is a ratio of observables of similar nature. Compared to the cross section, the asymmetry is thus significantly less affected by the scale and PDF uncertainties. One is then mainly left only with the experimental uncertainties in the determination of the cross sections and with the measurement of the polarisation of the top quarks⁴. In the MSSM, the asymmetry will nevertheless remain sensitive to the electroweak and strong radiative corrections from supersymmetric particles which also strongly affect the cross sections at high $\tan\beta$ values [7, 15, 16].

The polarisation asymmetry in tH^- associated production has been discussed in Ref. [17], following an original study of the asymmetry in the case of associated top–charged slepton production in the MSSM [18]. A detailed analysis of the top polarisation in $bg \rightarrow tH^-$ production has also been given in Ref. [10] which provides material that partly overlaps with the one presented here.

In the next section, we discuss this asymmetry in the Born approximation and exhibit its dependence on $\tan\beta$. In section 3, we show that it is essentially independent of the scale and PDF choices but remains dependent on the important SUSY radiative corrections that occur in the MSSM. A brief conclusion is given in section 4.

2. The A_{LR}^t asymmetry at tree–level

The starting point is the partonic process

$$b(p_b, \lambda_b) g(p_g, \lambda_g) \rightarrow t(p_t, \lambda_t) H^-(p_H). \quad (4)$$

The momentum (helicity) of the particle i is denoted by p_i (λ_i). In the Born approximation the process is mediated by two Feynman diagrams, one with s –channel bottom quark exchange and another with u –channel top quark exchange. In the case of type II 2HDM couplings the

³This asymmetry shares common interesting features with the long celebrated A_{LR} asymmetry for fermion pair production in longitudinally polarized electron–positron annihilation on the Z pole [13].

⁴We will not address here the issue of the experimental determination of the top quark polarisation from analyses of kinematical distributions of its decay products. For a detailed discussion, see for instance, Ref. [14].

helicity amplitude $F_{\lambda_b \lambda_g \lambda_t}$ reads as follows [9]

$$\begin{aligned}
F_{\lambda_b \lambda_g \lambda_t} &= \frac{gg_s \lambda^l \sqrt{x_+}}{2M_W} \left\{ \frac{\delta_{\lambda_b \lambda_g}}{\sqrt{\hat{s}}} \left[\lambda(1-r_t) s_{\theta/2} \delta_{\lambda_b \lambda_t} + \frac{1+r_t}{2} c_{\theta/2} \delta_{\lambda_b - \lambda_t} \right] \right. \\
&+ \frac{m_t \delta_{\lambda_b \lambda_g}}{\hat{u} - m_t^2} \left[(1+r_t) s_{\theta/2} \lambda \delta_{\lambda_b \lambda_t} + \frac{1-r_t}{2} c_{\theta/2} \delta_{\lambda_b - \lambda_t} \right] \\
&+ \frac{(1-r_t) s_{\theta/2} \lambda \delta_{\lambda_b \lambda_t}}{\hat{u} - m_t^2} [-p(1+c_\theta) \delta_{\lambda_b - \lambda_g} + d_t \delta_{\lambda_b \lambda_g}] \\
&+ \left. \frac{(1+r_t) c_{\theta/2} \delta_{\lambda_b - \lambda_t}}{2(\hat{u} - m_t^2)} [p(1-c_\theta) \delta_{\lambda_b - \lambda_g} + d_t \delta_{\lambda_b \lambda_g}] \right\} [m_t \cot \beta \delta_{\lambda_t L} + m_b \tan \beta \delta_{\lambda_t R}]. \quad (5)
\end{aligned}$$

The partonic Mandelstam variables are defined as $\hat{s} = (p_b + p_g)^2$ and $\hat{u} = (p_b - p_H)^2$. The angle θ is the azimuthal angle in the center-of-mass frame, while g_s is the strong coupling constant. The abbreviations d_t , r_t , x_\pm and λ read as follows

$$d_t = \sqrt{\hat{s}} - E_t + p \cos \theta, \quad r_t = \sqrt{\frac{x_-}{x_+}}, \quad x_\pm = \left(\sqrt{\hat{s}} \pm m_t \right)^2 - M_{H^\pm}^2, \quad (6)$$

$$\lambda = \sqrt{(1 - (x_t + x_h)^2)(1 - (x_t - x_h)^2)},$$

while $p \equiv |\mathbf{p}_t|$, $c_\alpha \equiv \cos \alpha$, and $s_\alpha \equiv \sin \alpha$. The partonic cross sections for L/R polarized top quarks in the final state is

$$\hat{\sigma}_{L/R} = \frac{p}{384\pi \hat{s}^{3/2}} \int_{-1}^{+1} d\cos \theta \sum_{\lambda_b, \lambda_g} |F_{\lambda_b \lambda_g L/R}|^2. \quad (7)$$

The integration over the angle θ leads to

$$\begin{aligned}
\hat{\sigma}_L &= \frac{GF\alpha_s}{24\sqrt{2}\hat{s}\lambda} \left\{ \lambda \left[m_t^2 \cot^2 \beta \left(\frac{7}{2} \lambda x_{ht}^2 + 2x_{ht}^2 + 2(1-x_{ht}^2)^2 + \frac{3}{2}(\lambda-1)\lambda \right) \right. \right. \\
&- m_b^2 \tan^2 \beta \left(-\frac{7}{2} \lambda x_{ht}^2 + 2x_{ht}^2 + 2(1-x_{ht}^2)^2 + \frac{3}{2}\lambda(\lambda+1) \right) \left. \right] + \\
&\Lambda \left[m_t^2 \cot^2 \beta \left((x_{ht}^2 + 2\lambda)(1-x_{ht}^2)^2 + (\lambda+1)(x_{ht}^2(\lambda+1)-1) \right) \right. \\
&+ m_b^2 \tan^2 \beta \left((2\lambda - x_{ht}^2)(1-x_{ht}^2)^2 + ((\lambda-1)x_{ht}^2 + 1)(1-\lambda) \right) \left. \right] \left. \right\}, \\
\hat{\sigma}_R &= \frac{GF\alpha_s}{24\sqrt{2}\hat{s}\lambda} \left\{ \lambda \left[m_b^2 \tan^2 \beta \left(\frac{7}{2} \lambda x_{ht}^2 + 2x_{ht}^2 + 2(1-x_{ht}^2)^2 + \frac{3}{2}(\lambda-1)\lambda \right) \right. \right. \\
&- m_t^2 \cot^2 \beta \left(-\frac{7}{2} \lambda x_{ht}^2 + 2x_{ht}^2 + 2(1-x_{ht}^2)^2 + \frac{3}{2}\lambda(\lambda+1) \right) \left. \right] + \\
&\Lambda \left[m_b^2 \tan^2 \beta \left((x_{ht}^2 + 2\lambda)(1-x_{ht}^2)^2 + (\lambda+1)(x_{ht}^2(\lambda+1)-1) \right) \right. \\
&+ m_t^2 \cot^2 \beta \left((2\lambda - x_{ht}^2)(1-x_{ht}^2)^2 + ((\lambda-1)x_{ht}^2 + 1)(1-\lambda) \right) \left. \right] \left. \right\}. \quad (8)
\end{aligned}$$

where $x_i = m_i/\sqrt{\hat{s}}$ and $x_{ht}^2 = x_h^2 - x_t^2$ and Λ is defined as

$$\Lambda = \log \left(\frac{1 - x_{ht}^2 + \lambda}{1 - x_{ht}^2 - \lambda} \right). \quad (9)$$

The total partonic cross section is then simply the sum of the cross sections $\hat{\sigma}_L$ and $\hat{\sigma}_R$

$$\hat{\sigma}_{\text{tot}} = \frac{G_F \alpha_s}{24\sqrt{2}\hat{s}} (m_t^2 \cot^2 \beta + m_b^2 \tan^2 \beta) \left\{ 2 [1 - 2x_{ht}^2 (1 - x_{ht}^2)] \Lambda - (3 - 7x_{ht}^2) \lambda \right\}. \quad (10)$$

As usual, these partonic cross sections have to be folded with the bottom–quark and gluon densities to obtain the hadronic ones σ_L, σ_R , and σ_{tot} . The expressions in the type I 2HDM can be obtained performing the substitution $m_b \tan \beta \rightarrow m_b \cot \beta$.

In Fig. 1 we display the left– and right– handed cross sections σ_L and σ_R as well as the asymmetry A_{LR}^t at the LHC as a function of $\tan \beta$. We choose two values of M_{H^\pm} , $M_{H^\pm} = 230$ and 412 GeV corresponding to the two 2HDMs scenarios of type II proposed in Refs. [15] (LS2) and [19] (SPS1a) respectively. The hadronic center-of-mass energy is fixed to $\sqrt{s} = 7$ TeV, and we adopt the CTEQ6L1 leading order PDFs [20] with $\alpha_s(M_Z^2) = 0.130$. The factorisation scale μ_F has been set to the value $\mu_0 = (M_{H^\pm} + m_t)/6$ which minimizes the higher order QCD corrections [7]. For the $H^- tb$ coupling, we use the on–shell top mass value $m_t = 173.1$ GeV and the $\overline{\text{MS}}$ mass of the bottom quark evaluated at a scale of $\mu = \mu_F$; in the SUSY scenario analyzed in this paper $m_b(\mu_F)$ ranges from 2.95 GeV to 3.10 GeV for all the values of μ_F considered.

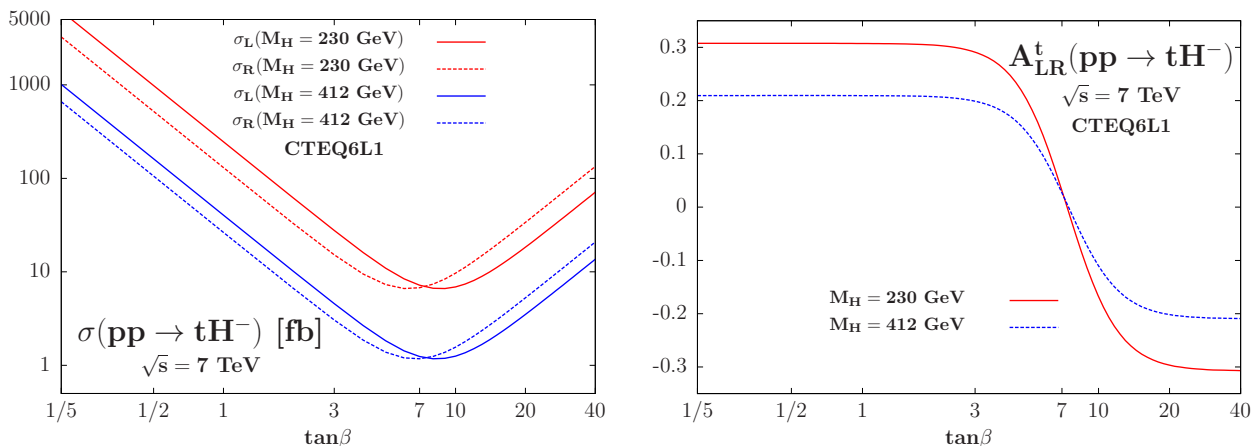


Figure 1: The cross sections σ_L and σ_R (left) and the asymmetry A_{LR} (right) at leading order in type II 2HDMs as a function of $\tan \beta$ in two benchmark scenarios with $M_{H^\pm} = 230$ and 412 GeV.

As can be seen σ_L and σ_R have the same order of magnitude: they are large at small $\tan \beta$ values, when the component $m_t \cot \beta$ of the $H^- tb$ coupling is significant, as well as at large $\tan \beta$ value when the $m_b \tan \beta$ component of the coupling is enhanced. The cross sections are equal and minimal at the value $\tan \beta = \sqrt{m_t/m_b} \simeq 7$ for which the $H^- tb$ coupling is the smallest. Therefore in type II 2HDM A_{LR}^t is maximal at low $\tan \beta$ values when the associated top quark is mostly left–handed and minimal at large $\tan \beta$ values when the top quarks are right handed. For a given value of the charged Higgs mass, the modulus of A_{LR}^t is the same in the $\tan \beta \gg 1$ and in the $\tan \beta \leq 1$ region. In the scenarios under consideration $|A_{LR}^t| = 0.31$ (0.21) for

$M_{H^\pm} = 230$ (412) GeV. The two $\tan\beta$ regions differ for the sign of the asymmetry. Therefore the sign of A_{LR}^t differentiates between the low and large $\tan\beta$ scenarios. In the intermediate $\tan\beta$ region, $\tan\beta \simeq 7$ for which $\sigma_L \simeq \sigma_R$, the asymmetry goes through zero.

In a type I 2HDM, the left- and right- components of the Yukawa coupling $g_{H^\pm tb}$ are both proportional to $\cot\beta$, and there is no $\tan\beta$ dependence in A_{LR}^t . The asymmetry is thus constant and is simply given by the A_{LR}^t value in the corresponding type II model evaluated at $\tan\beta = 1$. For type I 2HDM characterized by $M_{H^\pm} = 230$ (412) GeV the value of A_{LR}^t can be read off Fig. 1, $A_{LR}^t = 0.31$ (0.21). Combining this value with the value of $\sigma_{\text{tot}} \propto \cot^2\beta$, the predictions of 2HDMs of type I and II can eventually be discriminated.

Note that while σ_L, σ_R and thus σ_{tot} strongly depend on the hadronic center-of-mass energy, the asymmetry dependence of A_{LR}^t is mild. The asymmetry is comparable for $\sqrt{s} = 7$ and 14 TeV. For instance at $\sqrt{s} = 14$ TeV in the type I model one obtains $A_{LR}^t = 0.27$ (0.18) for $M_{H^\pm} = 230$ (412) GeV.

3. Scale and PDF dependence and impact of the NLO corrections

In this paper, the asymmetry A_{LR}^t has been evaluated at tree-level. The yet uncalculated higher order QCD contributions on this observable can be estimated from its dependence on the factorisation scale μ_F at which the process is evaluated. Starting from our reference scale μ_0 we vary μ_F within the range $\mu_0/\kappa \leq \mu_F \leq \kappa\mu_0$ with the constant factor chosen to be $\kappa = 2, 3$ or 4. The left panel of Fig. 2 shows the variation of the polarisation asymmetry for the choices $\kappa = 2, 3$ and 4. The insert shows the scale variation relative to the asymmetry value when the central scale is adopted. As one can see the scale dependence is very mild. In the low and in the high $\tan\beta$ region, it is at most at the level of 2%, even for $\kappa = 4$. At moderate values of $\tan\beta$, $\tan\beta \simeq 7$, the relative variation is much larger since the asymmetry vanishes. However the absolute impact of the scale variation is comparable to the one obtained for low and high $\tan\beta$ values, and thus small in absolute terms. It is worth to notice that the NLO QCD total cross section σ_{tot} exhibits a bigger residual scale uncertainty estimated to be of the order of 10–20% at the LHC with $\sqrt{s} = 7$ TeV [21].

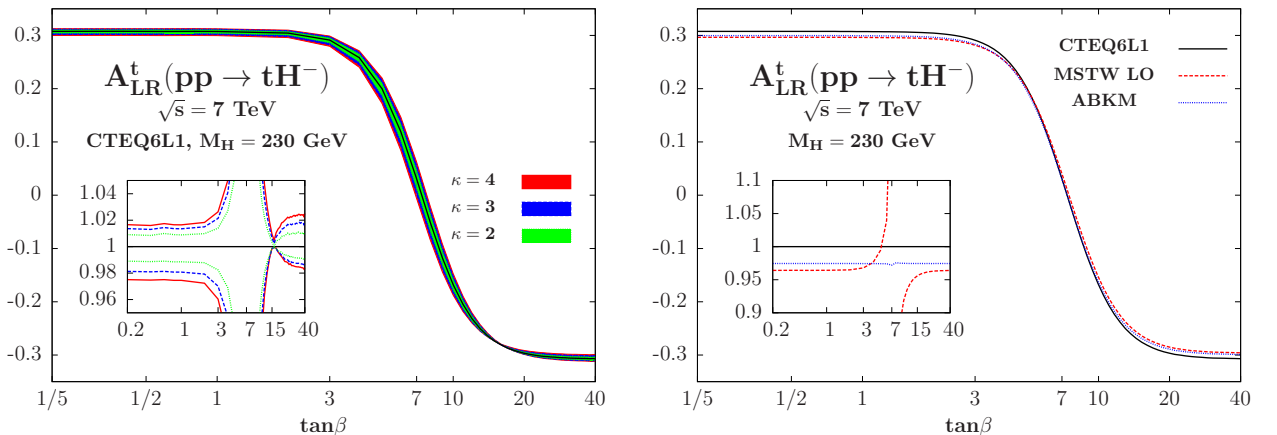


Figure 2: The scale variation (left) and the PDF dependence (right) of the asymmetry A_{LR}^t at leading order at the LHC with $\sqrt{s} = 7$ TeV as a function of $\tan\beta$. We consider the type II 2HDM characterized by $M_{H^\pm} = 230$ GeV. In the inserts, shown are the variations with respect to the central value.

Another source of uncertainty stems from the presently not satisfactory determination of the gluon and bottom quark PDFs. We estimate this type of uncertainty evaluating the asymmetry with several PDF parameterizations. In the right panel of Fig. 2 we show the dependence of the asymmetry on $\tan\beta$ when the CTEQ, the MSTW [22], and the ABKM [23] PDF sets are used. We consider the type II 2HDM characterized by $M_{H^\pm} = 230$ GeV. As usual the asymmetry has been computed at the LHC with $\sqrt{s} = 7$ TeV. In the insert we show the relative deviation from the CTEQ central prediction. As can be seen, the difference between the various predictions is rather small, less than few percents at low and high $\tan\beta$ values. The peaks in the insert for $\tan\beta \simeq 7$ correspond to the vanishing of A_{LR}^t . The effect of the PDF variation on the total cross section σ_{tot} is expected to be much larger. For instance at NLO the PDF uncertainty is expected to be of the order of 10% [21].

A final remark has to be made on the radiative corrections in supersymmetric scenarios. In the MSSM, the process (4) is affected by radiative corrections involving the supersymmetric particle spectrum. The NLO QCD and electroweak corrections have been discussed in Ref. [7] and in Ref. [15] respectively. Some of these corrections are known to be large for high values of $\tan\beta$ and some other parameters such as the higgsino mass parameter μ . It turns out that the bulk of these radiative corrections can be accounted for modifying the Yukawa coupling (2) as described in Ref. [16]. This modification is equivalent of using an effective bottom–quark mass. The approximation is rather good for the SUSY–QCD corrections (in particular when the SUSY spectrum is rather heavy), and slightly worse in the case of the electroweak ones.

In Fig. 3, we display the impact of these NLO SUSY radiative corrections within the MSSM on both the total cross section and the left–right asymmetry as a function of $\tan\beta$. The other SUSY parameters are fixed according to the scenario presented in Ref. [15], characterized by a heavy superparticle spectrum and $M_{H^\pm} = 270$ GeV. The SUSY QCD corrections are included in the approximation of Ref. [16], while the electroweak and the (very small) QED corrections are computed exactly. In the $\tan\beta$ range considered the approximation for the SUSY QCD contributions is expected to be valid.

As can be seen, the NLO corrections can be large in both the cross section and the asymmetry. In the case of the latter observable the effect is of the order of 10% in the $\tan\beta \geq 15$ region, where the asymmetry dependence on $\tan\beta$ is almost flat. Therefore the asymmetry is sensitive to the quantum contributions of the superparticle spectrum. A precise measurement of the asymmetry could allow to probe these additional supersymmetric corrections and, hence, could help to discriminate between supersymmetric and non–supersymmetric 2HDM of type II.

4. Conclusion

In the process of tH^- associated production at the LHC, the left–right asymmetry, eq. (3), obtained by identifying the polarisation of the top quarks is rather stable against the scale and PDF variation. It is still sensitive to quantum effects in new physics scenarios such as Supersymmetry. If measured with some accuracy, the top quark polarisation asymmetry in this process allows a very nice determination of the parameter $\tan\beta$. The combined measurement of the production cross section and the polarisation asymmetry could discriminate between various new physics scenarios: two–Higgs doublet models of type I versus type II and the MSSM versus non-supersymmetric models, at least for intermediate values of $\tan\beta$. For $\tan\beta \gg 1$ or

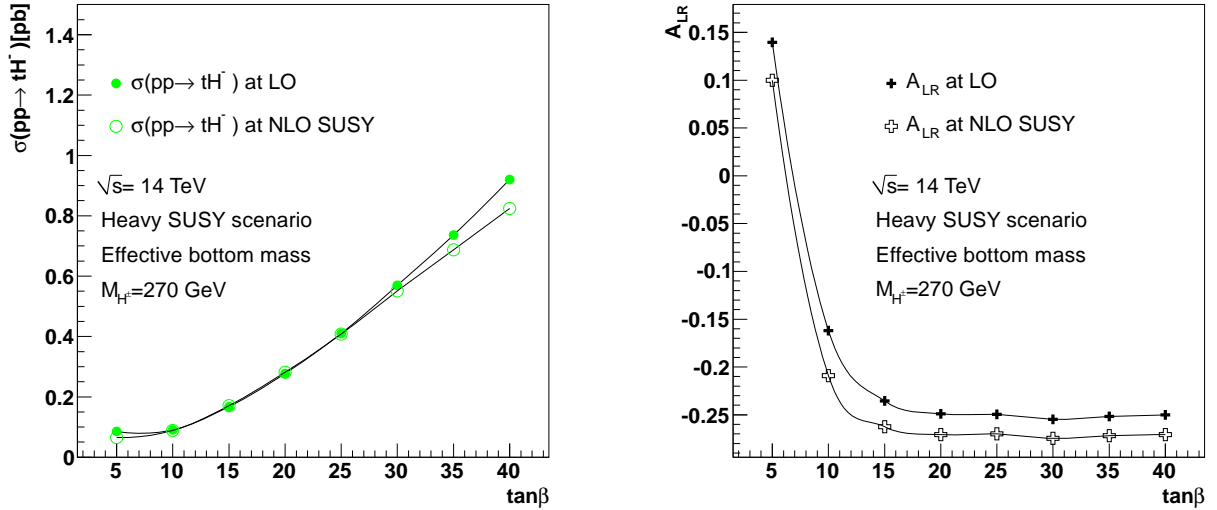


Figure 3: The total production cross section (left) and the asymmetry A_{LR}^t (right) at leading order and including the NLO SUSY corrections at the LHC with $\sqrt{s} = 14$ TeV. We consider the MSSM scenario of Ref. [15] characterized by a heavy sparticle spectrum and $M_{H^\pm} = 270$ GeV. $\tan\beta$ is varied from 5 to 40.

$\tan\beta \leq 1$ the method allows for the determination of the region of $\tan\beta$ but not for the exact value of $\tan\beta$, since in this two regions A_{LR}^t has a plateau. Note also that in the $\tan\beta \leq 1$ region the predictions for the asymmetry in the THDM I and II coincide. This polarisation asymmetry is thus worth investigating theoretically and experimentally in more detail.

Acknowledgments. Discussions with Rohini Godbole and Tilman Plehn are acknowledged. The work of A.D. is supported by the ERC Grant “Mass Hierarchy and Particle Physics at the TeV Scale” and the project ANR CPV-LFV-LHC NT09-508531. E.M. is supported by the European Research Council under Advanced Investigator Grant ERC-AdG-228301.

References

- [1] J.F. Gunion, H.E. Haber, G.L. Kane and S. Dawson, “The Higgs Hunter’s Guide”, Addison–Wesley, Reading (USA), 1990; G.C. Branco, P.M. Ferreira, L. Lavoura, M.N. Rebelo, Marc Sher and Joao P. Silva, arXiv:1106.0034 [hep-ph].
- [2] For a review of the MSSM Higgs sector: A. Djouadi, Phys. Rept. 459 (2008) 1.
- [3] G. L. Bayatian *et al.* [CMS Collaboration], J. Phys. G **G34**, 995-1579 (2007); G. Aad *et al.* [ATLAS Collaboration], JINST **3**, S08003 (2008).
- [4] D. Dicus and S. Willenbrock, Phys. Rev. D39 (1989) 751; R. Harlander and W. Kilgore, Phys. Rev. D68 (2003) 013001; H. Georgi et al. Phys. Rev. Lett. 40 (1978) 692; M. Spira et al., Phys. Lett. B318 (1993) 347; M. Spira et al., Nucl. Phys. B453 (1995) 17.

- [5] R. Kinnunen, S. Lehti, F. Moortgat, A. Nikitenko and M. Spira in Proceedings of the Les Houches Workshop on “Physics at TeV Colliders”, hep-ph/0406152.
- [6] J.F. Gunion, H. Haber, F. Paige, W.K. Tung and S. Willenbrock, Nucl. Phys. B294 (1987) 621; F. Borzumati, J.L. Kneur and N. Polonsky, Phys. Rev. D60 (1999) 115011.
- [7] T. Plehn, Phys. Rev. D67 (2003) 014018; S. Zhou, Phys. Rev. D67 (2003) 075006.
- [8] For reviews of charged Higgs physics, see: D.P. Roy, Mod. Phys. Lett. A19 (2004) 1813; S. Moretti, Pramana 60 (2003) 369; A. Djouadi, Int. J. Mod. Phys. A10 (1995) 1.
- [9] M. Beccaria, F.M. Renard and C. Verzegnassi, Phys. Rev. D71 (2005) 033005.
- [10] K. Huitu et al., JHEP 1104 (2011) 026.
- [11] K. Nakamura et al., J. Phys. G37 (2010) 075021.
- [12] J. Baglio and A. Djouadi, JHEP 1103 (2011) 055; arXiv:1103.6247 [hep-ph].
- [13] See for instance, B. Lynn and C. Verzegnassi, Phys. Rev. D35 (1987) 3326; A. Blondel, B. Lynn, F.M. Renard and C. Verzegnassi, Nucl. Phys. B304 (1988) 438.
- [14] M. Beneke, I. Efthymiopoulos, M.L. Mangano and J. Womersley (conv.) et al., hep-ph/0003033; W. Bernreuther, J. Phys. G35 (2008) 083001; R.M. Godbole, K. Rao, S.D. Rindani and R.K. Singh, JHEP 1011 (2010) 144; AIP Conf. Proc. 1200 (2010) 682.
- [15] M. Beccaria et al., Phys. Rev. D80 (2009) 053011.
- [16] See e.g., M. Carena et al., Nucl. Phys. B577 (2000) 88; D. Noth and M. Spira, Phys. Rev. Lett. 101 (2008) 181801 and references therein.
- [17] C. Verzegnassi, talk given at the Workshop, ”Charged Higgs”, Uppsala, September 2010; <http://www.grid.tsl.uu.se/chargedhiggs2010/>.
- [18] M. Akai, K. Huitu, S.K. Rai and K. Rao, JHEP 1008 (2010) 082.
- [19] B.C. Allanach et al., Eur. Phys. J. C25 (2002) 113.
- [20] P.M. Nadolsky et al. (CTEQ coll.), Phys. Rev. D78 (2008) 013004.
- [21] S. Dittmaier et al., “Handbook of LHC Higgs cross sections”, arXiv:1101.0593 [hep-ph].
- [22] A.D. Martin, W. Stirling, R. Thorne and G. Watt, Eur. Phys. J. C63 (2009) 189.
- [23] S. Alekhin et al., Phys. Rev. D81 (2010) 014032.